

RESEARCH ARTICLE | FEBRUARY 14 2022

Optimal design and trajectory tracking experiment of a novel 3-DOF parallel antenna mechanism

Guoxing Zhang; Xinlu Xia; Yulei Hou; Jinwei Guo ; Jianliang He; Chong Li



AIP Advances 12, 025321 (2022)

<https://doi.org/10.1063/5.0079915>



View
Online



Export
Citation



APL Energy
Latest Articles Online!

Read Now



Optimal design and trajectory tracking experiment of a novel 3-DOF parallel antenna mechanism

Cite as: AIP Advances 12, 025321 (2022); doi: 10.1063/5.0079915

Submitted: 25 November 2021 • Accepted: 27 January 2022 •

Published Online: 14 February 2022



View Online



Export Citation



CrossMark

Guoxing Zhang,¹ Xinlu Xia,¹ Yulei Hou,² Jinwei Guo,^{1,a)} Jianliang He,¹ and Chong Li¹

AFFILIATIONS

¹ School of Mechanical Engineering, Jiangsu University of Science and Technology, Zhenjiang 212100, China

² School of Mechanical Engineering, Yanshan University, Qinhuangdao 066004, China

^{a)}Author to whom correspondence should be addressed: 1473733099@qq.com

ABSTRACT

The tracking range and pointing performance of the antenna are important indices to measure the antenna system. First, the 3 degree of freedom parallel mechanism is proposed for the supporting mechanism of the antenna. The trajectory tracking principle of the antenna mechanism is analyzed based on the inverse position solution model. Meanwhile, the kinematic model of the antenna mechanism with a specific motion trajectory is derived. In addition, the structural optimization design is demonstrated based on the actuation torques and motion range index. In addition, the trajectory planning research is carried out according to the trajectory tracking requirements. The trajectory planning simulation is carried out in the joint space. Afterward, the antenna motion range is obtained through simulation. The specific trajectory tracking simulation of the antenna is completed. Furthermore, the pitch and azimuth motion performance experiments are carried out based on the developed antenna mechanism prototype. Finally, the pentagram trajectory tracking performance is verified via experiments. This research serves as a reference for designing and engineering application of the antenna.

© 2022 Author(s). All article content, except where otherwise noted, is licensed under a Creative Commons Attribution (CC BY) license (<http://creativecommons.org/licenses/by/4.0/>). <https://doi.org/10.1063/5.0079915>

I. INTRODUCTION

Antennas are widely used in signal communication and military investigation. The antenna mechanism is the carrier of stable and reliable operation of the antenna system. The parallel mechanism consists of multiple legs and closed chains, which has the characteristics of compact structure, excellent bearing performance, low inertia, and small error accumulation.¹ The parallel antenna has significant research value and application potential in avoiding the blind area of detection, improving the stability of system operation, and broadening the new configuration of the antenna mechanism.

The AMiBA radio telescope adopts the Stewart parallel mechanism as the supporting mechanism of the telescope. There are 13 groups of 1.2 m aperture antenna arrays of the supporting mechanism of the radio telescope.² The Stewart parallel mechanism is used for the attitude adjustment of the secondary reflector of the Tianma telescope.^{3,4} The 500-m aperture spherical radio telescope (FAST)

system includes the active reflector, feed cabin, feed cabin attitude adjustment device, and measurement and control device, becoming the world's largest and most sensitive radio telescope.⁵ Deng *et al.*⁶ designed a geodesic grid method for dividing the reflector of the ring truss antenna.

The trajectory tracking task needs to realize the azimuth and pitch movements. In addition, taking into account the storage requirements of the antenna system, the less degree of freedom (DOF) parallel mechanism can also meet the movement requirements of the antenna system. Li *et al.*⁷ designed a 2-DOF redundantly driven parallel antenna mechanism. Based on the kinematic model, the workspace and singularity of the mechanism were studied. Lauren *et al.*⁸ designed a 3-DOF antenna pointing mechanism and analyzed its pointing accuracy. Xu *et al.*⁹ applied the 2RPU-UPR parallel mechanism with two continuous rotation shafts to the antenna field, completed the optimization design, and made the prototype. Zhang¹⁰ carried out the research on debugging and

calibration method of the polar axis antenna supporting mechanism. Altuzarra *et al.*¹¹ designed a parallel pointing mechanism for solar tracking. Abid *et al.*¹² studied the stiffness performance of a new 2-DOF fast pointing static mechanism. Ahi and Haeri¹³ studied the dynamic modeling and control of a pitch and yaw guidance mechanism. Kumar and Natarajan measured the pointing accuracy of the antenna system using the laser tracker.¹⁴ Corinaldi *et al.*¹⁵ studied the singularity free path planning problem of the 3-CPU (C and U represent cylinder and universal joints, respectively) parallel pointing mechanism. Shao *et al.*¹⁶ completed the structure and controller design of the antenna reflector piezoelectric actuation directional station. Zhang *et al.*¹⁷ studied the kinematics and dynamics of a 4-DOF parallel antenna. Guo *et al.*¹⁸ proposed a new modular truss deployable antenna mechanism and carried out the combination method and performance analysis. Zou *et al.*¹⁹ developed a 3-DOF parallel manipulator with no rotational capacity. Chu *et al.*²⁰ proposed a planar antenna mechanism composed of planar multi-link deployable units. Feng and Liu²¹ proposed a design method of the deployable antenna reflector based on graph theory. Song *et al.*²² studied the synthesis of the parallel antenna mechanism based on the displacement subgroup and displacement manifold and proposed two new parallel antenna mechanisms with two rotational DOFs. Han *et al.*²³ investigated the configuration synthesis of a ring truss deployable mechanism for space antennas based on screw theory. Guo *et al.*²⁴ proposed a novel method based on symmetric hexagonal division and its corresponding modular truss deployable antenna mechanism. Majeed *et al.*^{25,26} proposed new Quadratic Trigonometric B-spline (QTBS) functions with two shape parameters, and they have been successfully applied in airplane design.

At present, the application of the parallel mechanism in the field of antenna is still in the stage of theoretical research and exploration. The trajectory tracking ability and pointing performance of the antenna system need to be further improved and optimized. It is an important research topic in the antenna field to design an antenna mechanism with a wide tracking range and good pointing performance. Therefore, a 3-DOF parallel mechanism with continuous motion is proposed to be applied for the antenna. In Sec. II, the pointing principle of the antenna mechanism is constructed. The trajectory tracking pointing model is established. In Sec. III, the trajectory planning of the antenna mechanism is studied. The structure is optimized according to the actuation torque and motion range index. In Sec. IV, the antenna pointing range is simulated and analyzed. Based on the experimental prototype, the motion performance and trajectory tracking of the antenna are developed. The main conclusions are presented in Sec. V.

II. POINTING PRINCIPLE ANALYSIS OF THE PARALLEL ANTENNA MECHANISM

A. Inverse kinematics of the parallel antenna mechanism

As shown in Fig. 1, the parallel antenna mechanism is composed of a moving platform, a fixed platform, and three branches. The three branches are connected with the fixed platform and the moving platform through rotation joints. The actuation angle of the rotation joint connected with the fixed platform is recorded as $\beta_i (i = 1, 2, 3)$. The fixed platform $P_1P_2P_3$ and the moving platform $Q_1Q_2Q_3$ are equilateral trigonal. Coordinate systems $O - xyz$ and

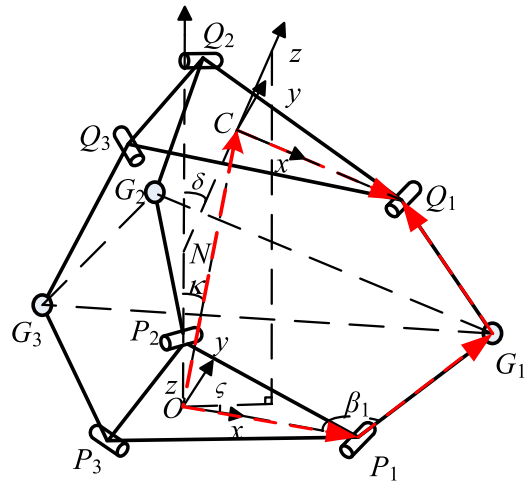


FIG. 1. Schematic diagram of the parallel antenna mechanism.

$C - xyz$ are established on the fixed/moving platform, respectively. The direction of the O_x axis is consistent with OP_1 , the direction of the O_z axis is perpendicular to the fixed platform and positive upward, the direction of the C_x axis is consistent with CQ_1 , and the direction of the C_z axis is perpendicular to the moving platform and positive upward. The relative distance between the origin vector OC of the fixed coordinate system and the moving coordinate system is r . The angle between the z -axis of the fixed coordinate system and the moving coordinate system is the pitch angle δ . The angle between the projection of the C_z axis of the moving coordinate system on the plane xoy and the fixed C_x axis is the azimuth angle ζ .

The actuation joint of the antenna mechanism comprises a rotation joint $P_i (i = 1, 2, 3)$ connected with the fixed platform. For inverse kinematic analysis, assume that the position matrix 0r and attitude matrix 0R_C of the motion platform are known. The purpose of inverse kinematics is to obtain the actuation joint variables. In order to obtain the angle value of each actuation joint, according to the structural characteristics of the antenna mechanism, the closed-loop vector equation of the branch can be written as

$${}^0OP_i + {}^0P_iG_i + {}^0G_iQ_i = {}^0r + {}^0R_C {}^CQ_i, \quad (1)$$

where $i = 1, 2$, and 3 , 0P_iG_i is the vector of the rotation joint P_i to G_i in the fixed coordinate system, 0G_iQ_i is the vector of the rotation joint G_i to Q_i in the fixed coordinate system, 0C_iQ_i is the vector of the rotation joint C_i to Q_i in the fixed coordinate system, and 0C_iQ_i is the vector of the rotation joint C_i to Q_i in the moving coordinate system.

According to the closed-loop vector equation, Eq. (1) can be expressed as

$${}^0G_iQ_i = {}^0r + {}^0R_C {}^CQ_i - {}^0OP_i - {}^0P_iG_i. \quad (2)$$

Relative to the fixed coordinate system, the position vector of moving the origin of the coordinate system can be expressed as ${}^0r = [r \sin \kappa \cos \zeta, r \sin \kappa \sin \zeta, r \cos \kappa]^T$. In addition, the pose

matrix ${}^0\mathbf{R}_C$ of the moving coordinate system can be expressed as

$${}^0\mathbf{R}_C = \begin{pmatrix} s^2\zeta v\delta + c\delta & -s\zeta c\zeta v\delta & c\zeta s\delta \\ -s\zeta c\zeta v\delta & c^2\zeta v\delta + c\delta & s\zeta s\delta \\ -c\zeta s\delta & -s\zeta s\delta & c\delta \end{pmatrix}, \quad (3)$$

where $s\zeta = \sin \zeta$, $c\zeta = \cos \zeta$, and $v\delta = 1 - \cos \delta$.

According to the constraint condition $|{}^0\mathbf{G}_i\mathbf{Q}_i| = L$ of the length, the following relation can be obtained:

$$(x_{Gi} - x_{Qi})^2 + (y_{Gi} - y_{Qi})^2 + (z_{Gi} - z_{Qi})^2 = L^2. \quad (4)$$

The relationship between the input and output of the parallel antenna mechanism is obtained as follows:

$$\theta_{11} = 2\arctg\left(\frac{4LA_3 + [16L^2A_3^2 - 4((A_1^2 + A_2^2 + A_3^2)^2 - 4L^2A_1^2)]^{\frac{1}{2}}}{2(A_1^2 + A_2^2 + A_3^2 - 2LA_1)}\right), \quad (5)$$

$$\theta_{21} = 2\arctg\left(\frac{4LB_3 + [16L^2B_3^2 - 4((B_1^2 + B_2^2 + B_3^2)^2 - (\sqrt{3}B_2L - B_1L)^2)]^{\frac{1}{2}}}{2(B_1^2 + B_2^2 + B_3^2 - (\sqrt{3}B_2L - B_1L))}\right), \quad (6)$$

$$\theta_{31} = 2\arctg\left(\frac{4LC_3 + [16L^2C_3^2 - 4((C_1^2 + C_2^2 + C_3^2)^2 - (\sqrt{3}C_2L + C_1L)^2)]^{\frac{1}{2}}}{2(C_1^2 + C_2^2 + C_3^2 + (\sqrt{3}C_2L - C_1L))}\right). \quad (7)$$

B. Trajectory tracking principle of the parallel antenna mechanism

The trajectory tracking principle of the mechanism is shown in Fig. 2. When the C_w axis of the moving coordinate system $C - C_u C_v C_w$ points to the target track point T , the target track can be tracked. Set the position vector $\mathbf{OT} = [T_x, T_y, T_z]^T$ of the target point T in the fixed coordinate system $O - O_x O_y O_z$, and set the distance from origin C of the moving coordinate system to the target point T as h .

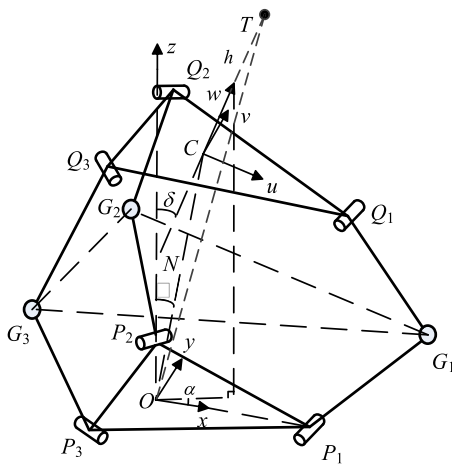


FIG. 2. Pointing diagram of the parallel antenna mechanism.

It is known that the vector of geometric center C of the moving platform to the fixed position is

$$\mathbf{OC} = [r \sin \kappa \cos \zeta, r \sin \kappa \sin \zeta, r \cos \kappa]^T. \quad (8)$$

The position coordinate of the target point T in the moving coordinate system $C - C_u C_v W_w$ is ${}^C\mathbf{CT} = [0, 0, h]^T$. In addition, the rotation matrix of the moving coordinate system $C - C_u C_v W_w$ relative to the fixed coordinate system $O - O_x O_y O_z$ is shown in Eq. (3). Therefore, the position vector of the target point T in the fixed coordinate system $O - O_x O_y O_z$ can be expressed as

$$\mathbf{OT} = {}^0\mathbf{R}_C {}^C\mathbf{CT} + \mathbf{CT}. \quad (9)$$

According to Eq. (9), the relationship between the position vector $\mathbf{OT} = [T_x, T_y, T_z]^T$ of the target point T in the fixed coordinate system $O - O_x O_y O_z$ and the pose parameters r, δ , and ζ of the parallel antenna can be obtained.

The trajectory of the mechanism is set to the pentagram pattern, as shown in Fig. 3. The local coordinate system $T_0 - xyz$ is set in the center of the pentagram. The coordinate vectors of points $A-E$ in the local coordinate system are $\mathbf{T}_0 T_A = [0, 0, 123.6]^T$, $\mathbf{T}_0 T_B = [0, 72.7, -100]^T$, $\mathbf{T}_0 T_C = [0, -117.5, 38.2]^T$, $\mathbf{T}_0 T_D = [0, 117.5, 38.2]^T$, and $\mathbf{T}_0 T_E = [0, -72.2, -100]^T$, respectively.

According to the experimental conditions, the local coordinate system $T_0 - xyz$ is given relative to the position vector $O - O_x O_y O_z$ in the fixed coordinate system,

$$\mathbf{OT}_0 = [-800, 0, 350]^T. \quad (10)$$

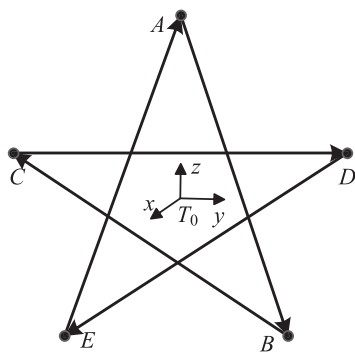


FIG. 3. Pentagram trajectory.

Thus, the position vector of the target trajectory points $A-E$ in the fixed coordinate system $O-O_xO_yO_z$ can be obtained as follows:

$$\mathbf{OT}_{A \sim E} = \mathbf{OT}_0 + \mathbf{T}_0 \mathbf{T}_{A \sim E} = [T_x, T_y, T_z]^T. \quad (11)$$

Substituting the coordinate vector of the target point into Eq. (11), the pose parameters r , δ , and ς of the parallel antenna varying with the target point can be obtained. Therefore, the actuation parameters of the parallel antenna can be obtained through the inverse kinematic solution.

C. Trajectory planning method

Trajectory planning is the premise to realize the effective control of the parallel antenna mechanism. The parallel antenna mechanism needs to realize the azimuth and pitch motions. In the process of motion, the motion node of the trajectory has the requirements of pose, velocity, and acceleration. The trajectory planning method of the quintic polynomial difference can be used in joint space to realize the trajectory planning of the parallel antenna. The quintic polynomial expression of the actuation joint angle is as follows:

$$\beta(t) = a_0 + a_1 t + a_2 t^2 + a_3 t^3 + a_4 t^4 + a_5 t^5. \quad (12)$$

The joint angular velocity $\dot{\beta}(t)$ and angular acceleration $\ddot{\beta}(t)$ are expressed as follows:

$$\begin{cases} \dot{\beta}(t) = a_1 + 2a_2 t + 3a_3 t^2 + 4a_4 t^3 + 5a_5 t^4, \\ \ddot{\beta}(t) = 2a_2 + 6a_3 t + 12a_4 t^2 + 20a_5 t^3. \end{cases} \quad (13)$$

The constraint conditions of the starting and ending points of the joint motion of the parallel antenna mechanism are as follows:

$$\begin{cases} \beta(0) = \beta_0, \beta(t_f) = \beta_f, \\ \dot{\beta}(0) = \dot{\beta}_0, \dot{\beta}(t_f) = \dot{\beta}_f, \\ \ddot{\beta}(0) = \ddot{\beta}_0, \ddot{\beta}(t_f) = \ddot{\beta}_f. \end{cases} \quad (14)$$

The simultaneous expressions (12)–(14) are as follows:

$$\begin{cases} \beta_0 = a_0, \beta_f = a_0 + a_1 t_f + a_2 t_f^2 + a_3 t_f^3 + a_4 t_f^4 + a_5 t_f^5, \\ \dot{\beta}_0 = a_1, \dot{\beta}_f = a_1 + 2a_2 t_f + 3a_3 t_f^2 + 4a_4 t_f^3 + 5a_5 t_f^4, \\ \ddot{\beta}_0 = 2a_2, \ddot{\beta}_f = 2a_2 + 6a_3 t_f + 12a_4 t_f^2 + 20a_5 t_f^3. \end{cases} \quad (15)$$

The coefficients of the quintic polynomial can be obtained based on solving Eq. (15),

$$\begin{cases} a_0 = \beta_0, a_1 = \dot{\beta}_0, a_2 = \frac{\ddot{\beta}_0}{2}, \\ a_3 = \frac{20\beta_f - 20\beta_0 - (8\dot{\beta}_f + 12\ddot{\beta}_0)t_f - (3\ddot{\beta}_0 - \ddot{\beta}_f)t_f^2}{2t_f^3}, \\ a_4 = \frac{30\beta_f - 30\beta_0 + (14\dot{\beta}_f + 16\ddot{\beta}_0)t_f + (3\ddot{\beta}_0 - 2\ddot{\beta}_f)t_f^2}{2t_f^4}, \\ a_5 = \frac{12\beta_f - 12\beta_0 - (6\dot{\beta}_f + 6\ddot{\beta}_0)t_f - (\ddot{\beta}_0 - \ddot{\beta}_f)t_f^2}{2t_f^5}. \end{cases} \quad (16)$$

III. STRUCTURE OPTIMIZATION AND SIMULATION OF THE PARALLEL ANTENNA MECHANISM

A. Structural optimization of the parallel antenna mechanism

The maximum value of branch actuation torque is related to the selection of servo motor. Further considering that the antenna completes the same trajectory, the motion range needs to be as small as possible. Therefore, the branch actuation torque and branch motion range are taken as the optimization indices. The parametric model of the mechanism is established using the ADAMS software. In addition, the structural parameters of the mechanism are optimized. The structural parameters of the mechanism include the connecting rod length L , fixed platform radius R_O , and moving platform radius R_C . The distance from the center of the moving platform to the center of the fixed platform is $|r|$. Therefore, L , R_O , R_C , and $|r|$ are selected as the design variables as shown in Table I.

According to the geometric structure of the mechanism and the initial value of design variables, 11 marking points are created in the Adams parametric analysis module, which are the fixed platform center point, moving platform center point, and 9 hinge points. The parametric equations of 11 marking points are completed according to the geometric characteristics. The design variables defined in Adams also include the rod length parameter L , initial height H , initial angles $Beta1$, $Beta2$, and $Beta3$, azimuth x , pitch angle d , fixed platform radius R_O_Varia , and moving platform radius R_C_Varia . The parametric model of the mechanism is shown in Fig. 4.

The comprehensive effect of four parameters on the actuation torque performance index of the mechanism is considered. Based on the experimental design function of parametric analysis, the optimization objectives and four groups of design variables are given. In addition, the design level is set to 6, that is, each group of design variables is divided into 6 groups of data. N groups of configuration

TABLE I. Parametric variables of the mechanism.

| Parameters | L (m) | R_O (m) | R_C (m) | $ r $ (m) |
|-----------------|-------------|-------------|-------------|-------------|
| Initial values | 0.420 | 0.150 | 0.150 | 0.520 |
| Variation range | 0.400–0.430 | 0.130–0.160 | 0.130–0.160 | 0.500–0.530 |

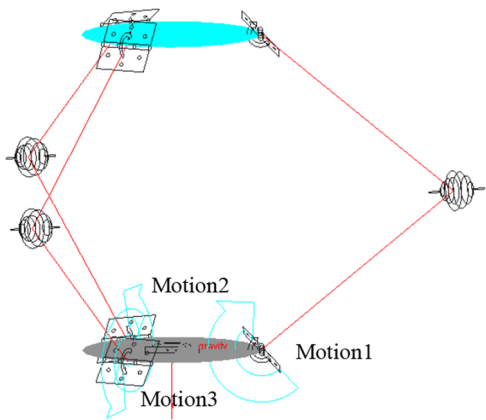


FIG. 4. Parametric model of the parallel antenna mechanism.

parameters are obtained, in which $N = 6^4 = 1296$. The relationship between each group of parameters and actuation torque obtained based on the experimental design module is shown in Fig. 5.

According to Fig. 5, the branch actuation torque fluctuates with the change in design variables. Select the smaller six groups of data in the maximum actuation torque of each branch in the simulation

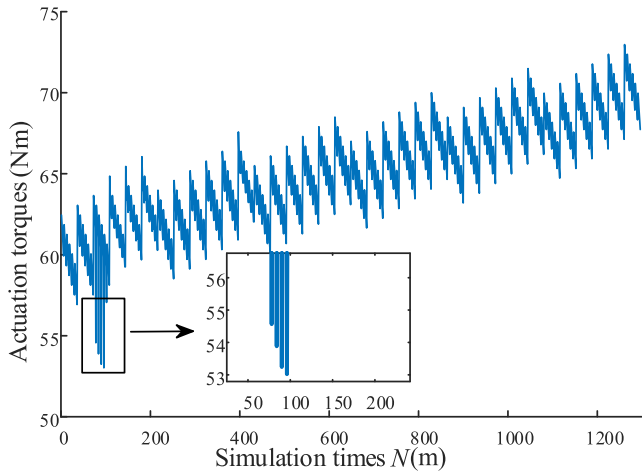


FIG. 5. Optimization results based on the actuation torque index.

TABLE II. Parametric variables based on the actuation torque index.

| N | L (m) | R_O (m) | R_C (m) | $ r $ (m) | Torques (N m) |
|-----|---------|-----------|-----------|-----------|---------------|
| 36 | 0.400 | 0.130 | 0.160 | 0.530 | 56.925 |
| 78 | 0.400 | 0.142 | 0.130 | 0.530 | 54.567 |
| 84 | 0.400 | 0.142 | 0.136 | 0.530 | 53.884 |
| 90 | 0.400 | 0.142 | 0.142 | 0.530 | 53.243 |
| 96 | 0.400 | 0.142 | 0.148 | 0.530 | 53.022 |

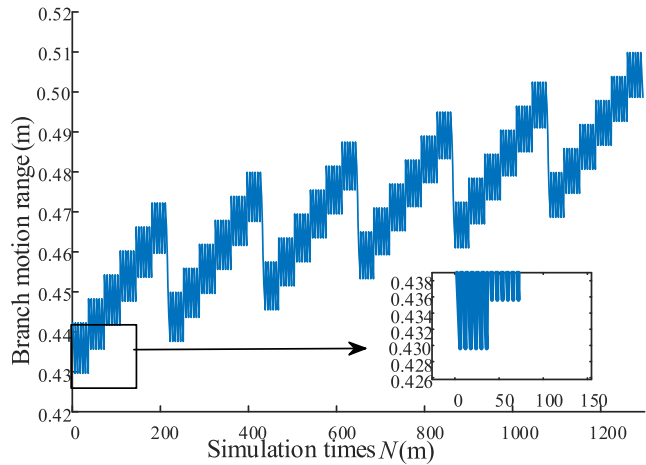


FIG. 6. Optimization results based on the branch motion range index.

TABLE III. Parametric variables based on the branch motion range index.

| N | L (m) | R_O (m) | R_C (m) | $ r $ (m) | Range (m) |
|-----|---------|-----------|-----------|-----------|-----------|
| 6 | 0.400 | 0.130 | 0.130 | 0.530 | 0.430 |
| 12 | 0.400 | 0.130 | 0.136 | 0.530 | 0.430 |
| 18 | 0.400 | 0.130 | 0.142 | 0.530 | 0.430 |
| 24 | 0.400 | 0.130 | 0.148 | 0.530 | 0.430 |
| 30 | 0.400 | 0.130 | 0.154 | 0.530 | 0.430 |
| 36 | 0.400 | 0.130 | 0.160 | 0.530 | 0.430 |

parameters, which are groups 36, 78, 84, 90, and 96, respectively. The values of five groups of parametric variables are shown in Table II.

The relationship between each group of parameters and the branch motion range obtained based on the experimental design module is shown in Fig. 6.

As shown in Fig. 6, the range of branch motion fluctuates with the change in design variables. Six groups of data with a small maximum branch motion range in the simulation parameters are taken out, which are groups 6, 12, 18, 24, 30, and 36, respectively. The values of six groups of parametric variables are shown in Table III.

According to Tables II and III, the actuation torque and branch motion range of the parallel mechanism are small in the 36th group of simulation parameters. Based on the experimental design and optimization analysis results, a set of key structural size parameters that make the mechanism have excellent performance is obtained. The connecting rod length of the mechanism is $L = 0.400$ m, the fixed platform radius is $R_O = 0.130$ m, the moving platform radius is $R_C = 0.160$ m, and the distance from the center of the moving platform to the fixed platform is $|r| = 0.530$ m.

B. Simulation analysis of the trajectory planning

The joint space quintic polynomial difference trajectory planning is simulated. The forms of azimuth and pitch motion of the parallel antenna mechanism are as follows: (1) azimuth motion: the pitch angle of the parallel antenna is 45° and the azimuth motion

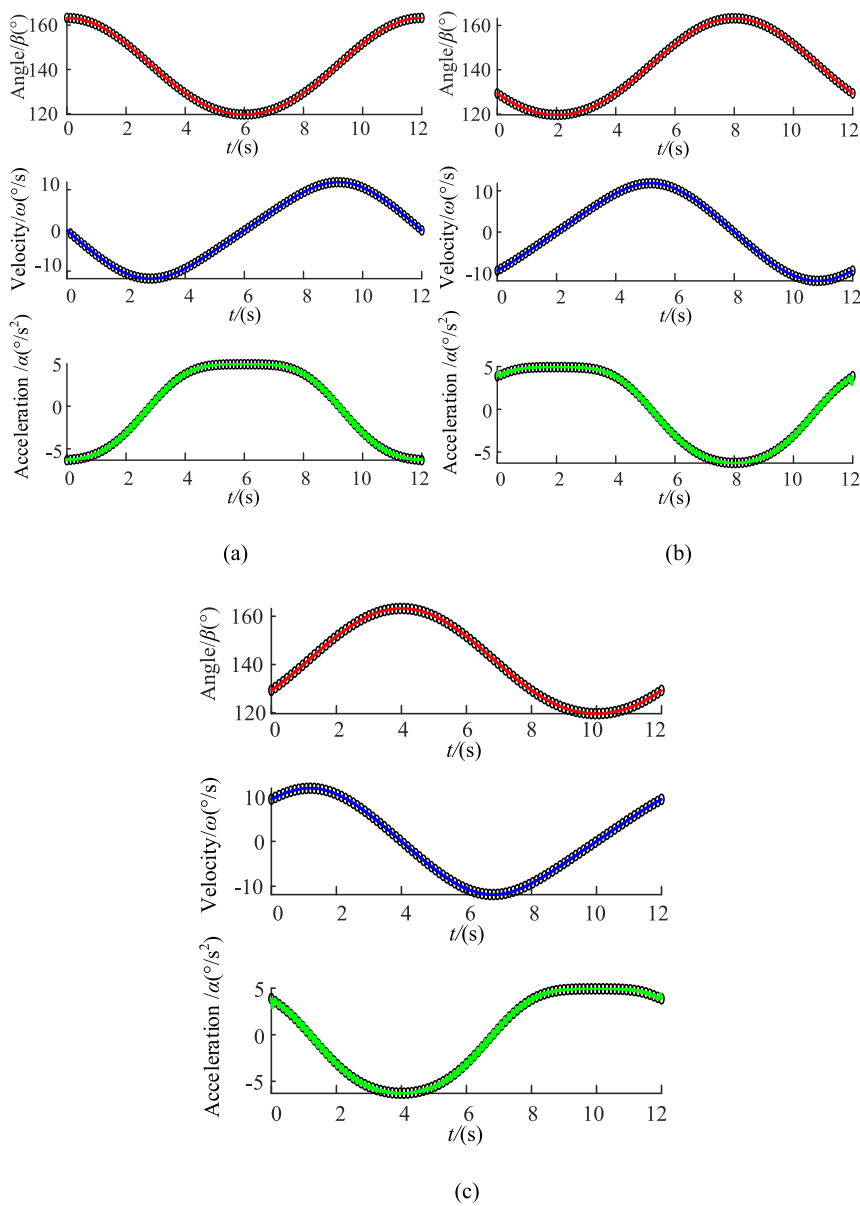


FIG. 7. Azimuth trajectory planning: (a) motion parameters of joint 1, (b) motion parameters of joint 2, and (c) motion parameters of joint 3.

is 0° – 360° at the speed of $30^\circ/\text{s}$ and (2) pitch motion: the azimuth angle of the parallel antenna is 0° and the pitch motion is 0° – 90° at the speed of $30^\circ/\text{s}$. The joint angle, angular velocity, and angular acceleration of the actuation joint of the parallel antenna mechanism are shown in Figs. 7 and 8.

As shown in Figs. 7 and 8, in the course of azimuth and pitch motion of the parallel antenna mechanism with a quintic polynomial difference, the trajectory curve of the actuation joint passes through all the target angular displacement, angular velocity, and angular acceleration nodes. The angular velocity and angular acceleration curves are smooth. In addition, the trajectory tracking process of the parallel antenna is stable. The quintic polynomial difference based

on joint space lays a foundation for the motion control of the parallel antenna.

C. Pointing performance simulation of the parallel antenna mechanism

The motion parameters of the parallel antenna mechanism are set as follows: (1) azimuth motion: azimuth angle $\zeta \in [0^\circ - 360^\circ]$, pitch angle $\delta = 45^\circ$, and relative distance $r = 540\text{mm}$, and (2) pitch motion: azimuth angle $\zeta = 0^\circ$, pitch angle $\delta \in [0^\circ - 90^\circ]$, and relative distance $r = 540\text{mm}$. MATLAB is used to simulate and verify the motion characteristics of the antenna mechanism, and the pitch and

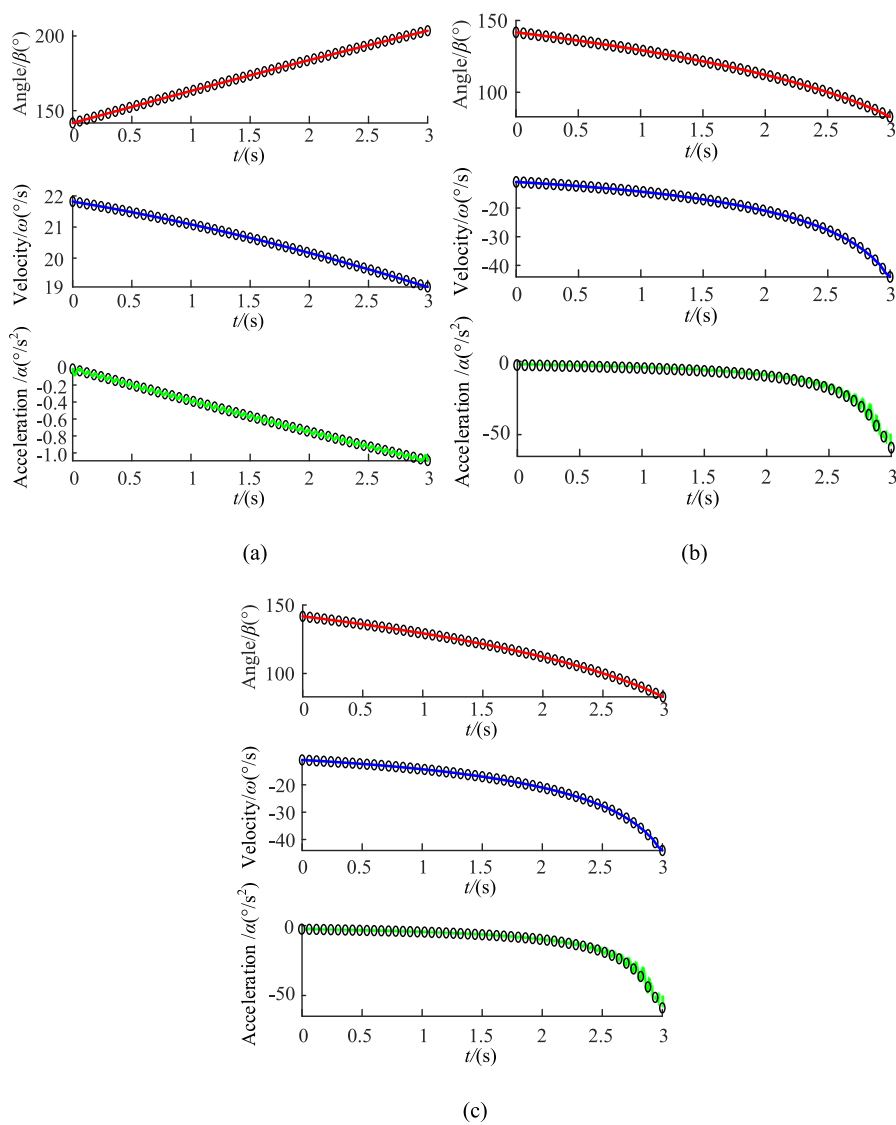


FIG. 8. Pitch trajectory planning: (a) motion parameters of joint 1, (b) motion parameters of joint 2, and (c) motion parameters of joint 3.

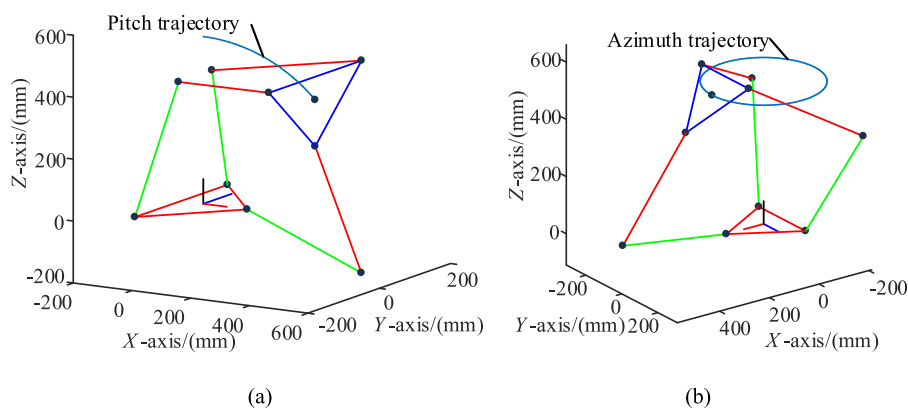


FIG. 9. Kinematic wireframe of the parallel antenna mechanism: (a) pitch motion and (b) azimuth motion.

azimuth motion trajectory and motion envelope space are obtained as shown in Figs. 9 and 10.

As shown in Figs. 9(a) and 9(b), the moving platform center motion trajectory is smooth. The parallel antenna system motion process is stable without interference. As shown in Fig. 10, the parallel antenna mechanism has the ability to move continuously in hemispherical space.

IV. EXPERIMENT ON THE POINTING PERFORMANCE OF THE PARALLEL ANTENNA MECHANISM

A. Pointing performance experiment

Considering the limitation of the range of motion of the antenna system in the experimental site, a ratio of 1:2 is used to make an experimental prototype of the parallel antenna mechanism to verify the trajectory tracking ability of the antenna mechanism. Based on the design of the parts, the assembly of the parts of the antenna mechanism is carried out by using SolidWorks, and the overall model of the antenna is finally obtained. Given the pitch angle, the movement posture demonstration of the parallel antenna mechanism is realized, as shown in Fig. 11.

Based on the three-dimensional configuration of the prototype, the experimental prototype is processed, assembled, and debugged. The physical prototype of the parallel antenna mechanism after assembly is shown in Fig. 12.

The antenna structure design and prototype development were carried out, and the electrical system and software system design were completed. Afterward, the performance of the antenna system is verified via the function test of the parallel antenna system. The pitch motion process of the parallel antenna mechanism is as follows: the starting pose is the initial pose, the expected pose is the



FIG. 12. Prototype of the parallel antenna mechanism.

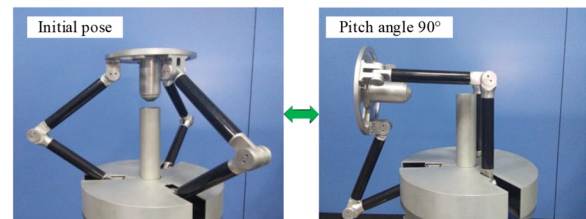


FIG. 13. Pitch process of the parallel antenna mechanism.

pitch specific angle pose, and the ending pose returns to the initial pose again. Figure 13 shows that the pitch angle is 90°.

The azimuth movement process of the parallel antenna mechanism is as follows: First, the antenna moves from initial attitude to azimuth angle 0° and pitch angle 45°. Second, the pitch angle of the antenna remains unchanged, and the azimuth angle moves from 0° to 180°. Third, the pitch angle of the antenna remains unchanged,

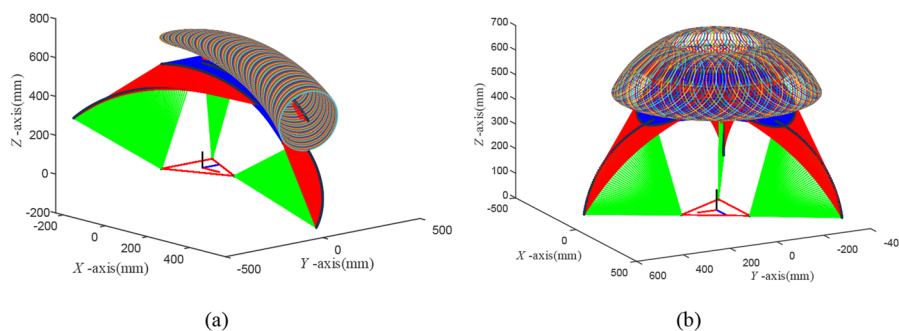


FIG. 10. Motion envelope of the parallel antenna mechanism: (a) pitch motion and (b) azimuth motion.

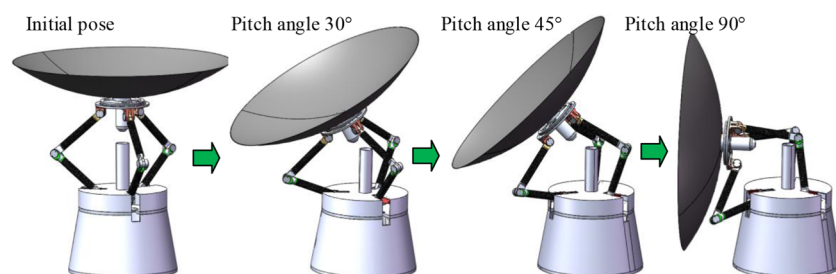


FIG. 11. 3D of the parallel antenna mechanism.

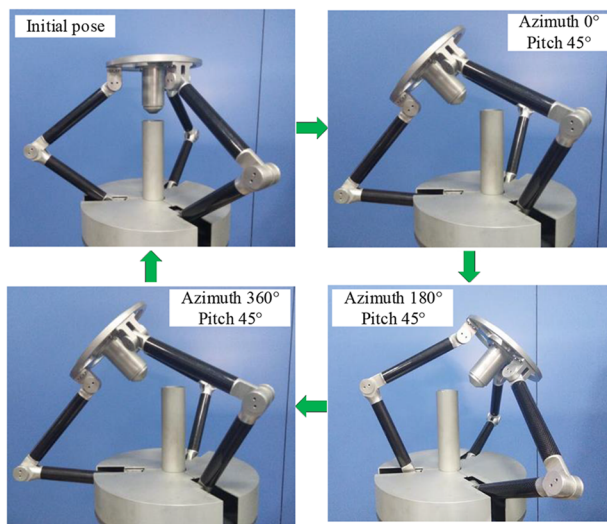


FIG. 14. Azimuth motion process of the parallel antenna mechanism.

and the azimuth angle moves from 180° to 360° . Finally, the initial position and orientation are returned from pitch angle 45° and azimuth angle 360° . The complete azimuth movement processes of the parallel antenna mechanism are shown in Fig. 14.

B. Trajectory tracking experiment

The purpose of the trajectory tracking experiment is to verify the trajectory tracking ability of the parallel antenna mechanism

and observe whether the parallel antenna mechanism can complete the action according to the expected trajectory. The contents of the experiment are as follows: The five pointed star pattern is given on the drawing board. The laser pen is used for preliminary calibration to determine the appropriate position of the drawing board. Then, the movement of the antenna is driven to make the laser beam emitted using the laser pen move along the pentagram trajectory.

Input the actuation data of the antenna position and orientation into the control program. The pentagram trajectory tracking experiment of the parallel antenna mechanism is shown in Fig. 15. The laser points on the moving platform of the 3-DOF parallel antenna move in the order of the pentagram pattern. The experimental results show that the 3-DOF parallel antenna can move in accordance with the expected target trajectory, showing good trajectory tracking ability.

The pointing accuracy is an important index to the parallel antenna mechanism. It is necessary to test the motion parameters of the parallel antenna mechanism by using measuring instruments. The Leica AT901-B laser tracker is adopted to observe the pitch and azimuth of the parallel antenna mechanism. After measuring the position and orientation of the moving coordinate system $C - C_u C_v C_w$ in the fixed coordinate system $O - O_x O_y O_z$ with the laser tracker, the actual values of the pitch angle δ and azimuth angle ζ of the parallel antenna mechanism are indirectly obtained. Table IV shows the pointing errors of the parallel antenna mechanism during the movement.

According to the measured data shown in Table IV, the trajectory tracking errors of azimuth and pitch angles after fitting are shown in Fig. 16.

As shown in Table IV and Fig. 16, the azimuth errors of the parallel antenna are maintained at -0.036° to 0.030° . The pitch errors

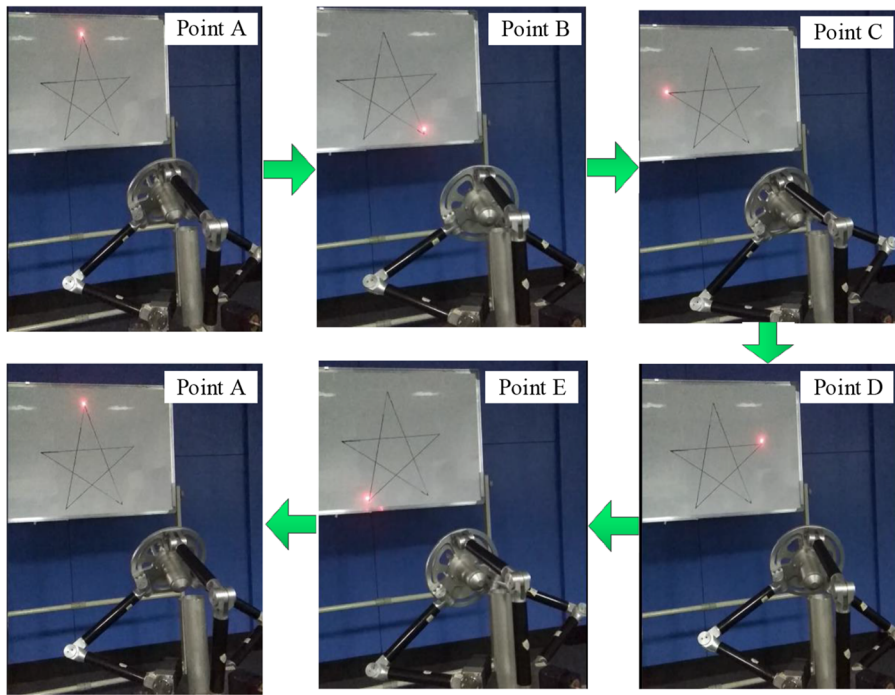
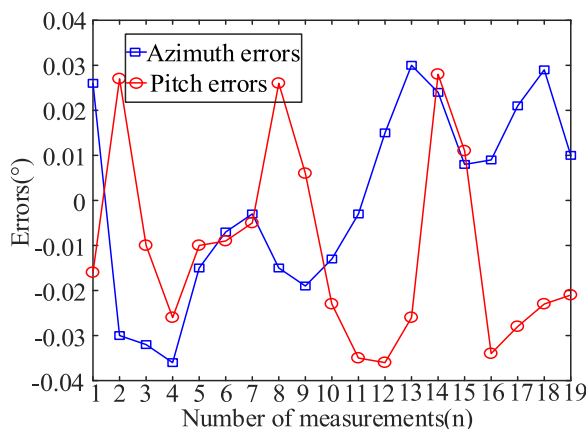


FIG. 15. Pentagram tracking process.

TABLE IV. Pointing errors of the parallel antenna mechanism.

| Azimuth ideal value (deg) | Azimuth actual value (deg) | Errors (deg) | Pitch ideal value (deg) | Pitch actual value (deg) | Errors (deg) |
|---------------------------|----------------------------|--------------|-------------------------|--------------------------|--------------|
| 0 | 0.026 | -0.026 | 30 | 29.984 | 0.016 |
| 20 | 19.970 | 0.030 | 30 | 30.027 | -0.027 |
| 40 | 39.968 | 0.032 | 30 | 29.990 | 0.010 |
| 60 | 59.964 | 0.037 | 30 | 29.974 | 0.026 |
| 80 | 79.985 | 0.015 | 30 | 29.990 | 0.010 |
| 100 | 99.993 | 0.007 | 30 | 29.991 | 0.009 |
| 120 | 119.997 | 0.003 | 30 | 29.995 | 0.005 |
| 140 | 139.985 | 0.015 | 30 | 30.026 | -0.026 |
| 160 | 159.981 | 0.019 | 30 | 30.006 | -0.006 |
| 180 | 179.987 | 0.013 | 30 | 29.977 | 0.023 |
| 200 | 199.997 | 0.003 | 30 | 29.965 | 0.035 |
| 220 | 220.015 | -0.015 | 30 | 29.964 | 0.036 |
| 240 | 240.030 | -0.03 | 30 | 29.974 | 0.026 |
| 260 | 260.024 | -0.024 | 30 | 30.028 | -0.028 |
| 280 | 280.008 | -0.008 | 30 | 30.011 | -0.011 |
| 300 | 300.009 | -0.009 | 30 | 29.966 | 0.035 |
| 320 | 320.021 | -0.021 | 30 | 29.972 | 0.028 |
| 340 | 340.029 | -0.029 | 30 | 29.977 | 0.023 |
| 360 | 360.010 | -0.010 | 30 | 29.979 | 0.021 |

**FIG. 16.** Trajectory tracking errors of the parallel antenna mechanism.

are maintained at -0.036° to 0.028° . The analysis shows that the pitch and azimuth pointing accuracy of the parallel antenna is better than 0.1° . The motion error of the parallel antenna is mainly caused by machining error and assembly error. From the experimental results, it can be inferred that the pointing accuracy of the parallel antenna meets the designing index.

V. CONCLUSIONS

The 3-DOF parallel mechanism is proposed as the antenna mechanism. The trajectory tracking principle of the parallel antenna

mechanism is deduced based on the inverse position model. Subsequently, the kinematic model of the parallel antenna mechanism with a specific motion trajectory is established. The structural parameters are optimized based on the branch actuation torque and motion range. In addition, the trajectory planning of the antenna is completed based on the quintic difference polynomial in the joint space. The antenna motion range is drawn based on software simulation. Moreover, the antenna specific trajectory tracking simulation is presented.

The prototype of the parallel antenna mechanism is developed, and the experimental research is carried out. The parallel antenna runs smoothly in the process of pitch and azimuth motion without interference. According to the trajectory tracking principle of the parallel antenna mechanism, the real-time tracking of the pentagram trajectory is realized. Furthermore, the effectiveness of the parallel antenna mechanism and control system is verified. The experimental results indicate that the pitch and azimuth pointing errors of the parallel antenna mechanism are less than 0.1° , which meets the design requirements. The research lays a foundation for engineering application of the parallel antenna mechanism.

ACKNOWLEDGMENTS

This study was financially supported by the National Key Research and Development Program of China (Grant No. 2018YFC0309100), the National Natural Science Foundation of China (Grant No. 51905228), the Hebei Natural Science Foundation (Grant No. E2019203109), and the Key Research Project in Higher Education Institutions of Hebei Province (Grant No. ZD2019020).

AUTHOR DECLARATIONS**Conflict of Interest**

The authors have no conflicts to disclose.

DATA AVAILABILITY

The data that support the findings of this study are available from the corresponding author upon reasonable request.

REFERENCES

- ¹Z. Huang, Q. C. Li, and H. F. Ding, *Theory of Parallel Mechanisms* (Springer, Dordrecht, 2013).
- ²P. M. Koch, M. Kesteven, H. Nishioka *et al.*, “The AMiBA hexapod telescope mount,” *Astrophys. J.* **694**(2), 1670–1684 (2009).
- ³Y. L. Hou, Y. B. Duan, Y. C. Dou *et al.*, “Calibration of adjusting mechanism for subreflector of a 65 meters radio telescope,” *China Mech. Eng.* **24**(24), 3318–3322+3328 (2013).
- ⁴J. T. Yao, D. X. Zeng, Y. L. Hou *et al.*, “Design and experiment research of sub-reflector adjusting system in large radio telescope antenna,” *Manned Spaceflight* **22**(1), 69–73+87 (2016).
- ⁵Q. Wang, Y. Gao, J. X. Xue *et al.*, “Key performance analysis of five-hundred-meter aperture spherical radio telescope reflective surface hydraulic actuator,” *J. Mech. Eng.* **53**(2), 183–191 (2017).
- ⁶H. Deng, T. Li, and Z. Wang, “Design of geodesic cable net for space deployable mesh reflectors,” *Acta Astronaut.* **119**, 13–21 (2016).
- ⁷X. Li, X. Ding, and G. S. Chirikjian, “Analysis of a mechanism with redundant drive for antenna pointing,” *Proc. Inst. Mech. Eng., Part G* **231**(2), 229–239 (2017).
- ⁸B. Lauren, R. Nicolas, and M. Yann, “3POD: A high performance parallel antenna pointing mechanism,” in *15th European Space Mechanisms and Tribology Symposium-ESMATS, Noordwijk, The Netherlands* (Noordwijk, 2013), pp. 25–27.
- ⁹Y. D. Xu, S. S. Tong, B. Wang *et al.*, “Application of 2RPU-UPR parallel mechanism in antenna support,” *China Mech. Eng.* **30**(14), 1748–1755 (2019).
- ¹⁰Y. L. Zhang, “Design of the pedestal of polar mount for solar radio observing system,” *Radio Commun. Technol.* **35**(5), 40–43 (2009).
- ¹¹O. Altuzarra, E. Macho, J. Aginaga *et al.*, “Design of a solar tracking parallel mechanism with low energy consumption,” *Proc. Inst. Mech. Eng., Part C* **229**(3), 566–579 (2015).
- ¹²M. Abid, J. Yu, Y. Xie *et al.*, “Conceptual design, modeling and compliance characterization of a novel 2-DOF rotational pointing mechanism for fast steering mirror,” *Chin. J. Aeronaut.* **33**(12), 3564–3574 (2020).
- ¹³B. Ahi and M. Haeri, “A high performance guidance filter scheme with exact dynamic modeling of a pitch yaw gimbaled seeker mechanism,” *Mech. Syst. Signal Process.* **144**, 106857 (2020).
- ¹⁴A. Kumar and T. Natarajan, “Laser based real time antenna pointing measurement system,” *Int. J. Eng. Technol.* **7**(3), 28–32 (2018).
- ¹⁵D. Corinaldi, M. Callegari, and J. Angeles, “Singularity-free path-planning of dexterous pointing tasks for a class of spherical parallel mechanisms,” *Mech. Mach. Theory* **128**, 47–57 (2018).
- ¹⁶S. Shao, Y. Shao, S. Song *et al.*, “Structure and controller design of a piezo-driven orientation stage for space antenna pointing,” *Mech. Syst. Signal Process.* **138**, 106525 (2020).
- ¹⁷G. X. Zhang, D. H. Zheng, J. W. Guo *et al.*, “Dynamic modeling and mobility analysis of the 3-R(RRR)R+R antenna mechanism,” *Robotica* **39**(8), 1485–1503 (2021).
- ¹⁸J. Guo, Y. Zhao, Y. Xu *et al.*, “A novel modular deployable mechanism for the truss antenna: Assembly principle and performance analysis,” *Aerospace Sci. Technol.* **105**, 105976 (2020).
- ¹⁹Q. Zou, D. Zhang, S. Zhang *et al.*, “Kinematic and dynamic analysis of a 3-DOF parallel mechanism,” *Int. J. Mech. Mater. Des.* **17**, 587 (2021).
- ²⁰Z. Chu, Z. Deng, X. Qi *et al.*, “Modeling and analysis of a large deployable antenna structure,” *Acta Astronaut.* **95**(1), 51–60 (2014).
- ²¹C. M. Feng and T. S. Liu, “A graph-theory approach to designing deployable mechanism of reflector antenna,” *Acta Astronaut.* **87**(6), 40–47 (2013).
- ²²Y. Song, Y. Qi, G. Dong, and T. Sun, “Type synthesis of 2-DOF rotational parallel mechanisms actuating the inter-satellite link antenna,” *Chin. J. Aeronaut.* **29**(6), 1795–1805 (2016).
- ²³B. Han, Y. Xu, J. Yao *et al.*, “Configuration synthesis of hoop truss deployable mechanisms for space antenna based on screw theory,” *AIP Adv.* **9**(8), 085201 (2019).
- ²⁴J. Guo, Y. Zhao, Y. Xu *et al.*, “Design and analysis of truss deployable antenna mechanism based on a novel symmetric hexagonal profile division method,” *Chin. J. Aeronaut.* **34**(8), 87–100 (2021).
- ²⁵A. Majeed, M. Abbas, F. Qayyum *et al.*, “Geometric modeling using new cubic trigonometric B-spline functions with shape parameter,” *Mathematics* **8**(12), 2102 (2020).
- ²⁶A. Majeed, M. Abbas, A. A. Sittar *et al.*, “Airplane designing using quadratic trigonometric B-spline with shape parameters,” *Mathematics* **6**(7), 7669–7683 (2021).